Frustrated antiferromagnetism and heavy-fermion-like behavior in PrPdAl

Zhen Wang [1,2] Hengcan Zhao,[1] Meng Lyu,[1] Junsen Xiang,[1] Yosikazu Isikawa [3] Shuai Zhang [1,2] and Peijie Sun [1,2,4,*]

[1]*Beijing National Laboratory for Condensed Matter Physics, Institute of Physics, Chinese Academy of Sciences, Beijing 100190, China*

[2]*School of Physical Science, University of Chinese Academy of Sciences, Beijing 100049, China*

[3]*Graduate School of Science and Engineering, University of Toyama, Toyama 930-8555, Japan*

[4]*Songshan Lake Materials Laboratory, Dongguan, Guangdong 523808, China*

(Received 14 October 2021; revised 22 February 2022; accepted 24 February 2022; published 11 March 2022)

We report on the long-range antiferromagnetic ordering with two successive phase transitions at $T_{N1} = 4.0$ K, $T_{N2} \approx 1.3$ K and the heavy-fermion-like behaviors in PrPdAl, a Kondo lattice with kagome-like structure of non-Kramers Pr ions in the hexagonal basal plane. The ground-state antiferromagnetism forms by two-thirds Pr ions with nearly full magnetic moment and one-third with strongly frustrated and reduced moment. The easy magnetization axis points along c whereas the ordered Pr $4f$ moments reside in the basal plane, mirroring the important effect of spin frustrations. The electronic specific-heat coefficient is strongly enhanced to $\sim$940 mJ/mol K^2, and the Kadowaki-Woods ratio is factor-of-25 smaller than that of conventional heavy-fermion compounds with Kramers doublet ground state. The effective Grüneisen ratio estimated from thermal expansion reveals large values in the vicinity of the broadened phase transition at T_{N2}, manifesting its instability against pressure. Accordingly, PrNiAl, a chemically pressurized analog of the titled compound, was found to reveal only one antiferromagnetic transition at a considerably higher temperature of 6.9 K. These results demonstrate that PrPdAl and related homologues can offer excellent cases for investigating competing ground states in frustrated Kondo lattices formed by non-Kramers magnetic ions.

DOI: 10.1103/PhysRevB.105.125113

I. INTRODUCTION

Geometrical frustration of local magnetic moments in correlated intermetallics is emerging as a new avenue to exotic quantum states at low temperatures [1–3]. The equiatomic ternary compounds RTX (R = rare earths, T = transition metals, X = Al, Ga or In) crystalizing in hexagonal ZrNiAl-type strucutre with space group $P\bar{6}2m$ are attracting increased attention in this context [4,5]. Here, magnetic frustration arises from a distorted-kagome lattice of R ions in the R-Ni basal layers, which are separated by nonmagnetic Ni-Al layers stacked long the c axis. Because the quantum fluctuations underpinned by geometrical frustration prevent the formation of not only long-range magnetic order, but also the Kondo singlet in the groud state [6], an array of exotic quantum phenomena may emerge from the competition of multiple relevant energy scales. These include, within the RXT family, an extended quantum critical phase observed in CePdAl [7], a non-Fermi liquid behavior in CeRhSn [8], and the multiple quantum critical points in YbAgGe [9]. Even in the absence of the Kondo effect, magnetic frustration in this family may lead to unconventional ground-state phenomena, e.g., the kagome spin ice state recently observed in HoAgGe [10].

Among the well-investigated RTX compounds, CePdAl provides a prominent case subject to the competition between magnetic frustration, Kondo effect, and the Ruderman-Kittel-Kasuya-Yosida (RKKY) interaction. Here, two-thirds Ce ions on the $3f$ sites, denoted as Ce(1) and Ce(3), order antiferromagnetically below 2.7 K with an incommensurate propagation vector $\mathbf{k} = [1/2, 0, 0.35]$ [11]. The remaining one-third Ce(2) is Kondo screened, giving rise to heavy-fermion behaviors with electronic specific-heat coefficient $\gamma = 270$ mJ/mol K^2 (see Refs. [12–14]). This unique partial antiferromagnetic ordering in CePdAl has been qualitatively interpreted by considering a ferromagnetic (J_1) nearest-neighbor (nn) and an antiferromagnetic (J_2) next-nearest-neighbor (nnn) exchange interaction between Ce moments in the basal plane, assuming the interlayer interactions are negligible [15]. Here the intralayer nn (nnn) Ce-Ce distance is 3.73 (5.25) Å, considerably shorter (longer) than the interlayer nn Ce-Ce distance, 4.24 Å (see Refs. [11,14]). Intriguingly, applying hydrostatic or chemical pressure to CePdAl suppresses the partial order and brings about an extended quantum critical phase, instead of a quantum critical point, in the zero-temperature pressure-field phase diagram [7].

Unlike CePdAl, PrPdAl was reported to exhibit two antiferromagnetic transitions at $T_{N1} = 4.0$ K and $T_{N2} \approx 1.5$ K [16]. However, neutron diffraction experiments performed at T_{N2} reveal a "partial" antiferromagnetic order in PrPdAl also, see Fig. 1, inset. Here, one-third of the magnetic moments at Pr(2) is reduced to 1.9 μ_B due to strong quantum spin fluctuations arising from frustration and presumably the Kondo effect as well, as compared to 3.1 μ_B at Pr(1) and Pr(3) that is close to the full magnetic moment of free Pr^{3+} ion [17]. This type of partial ordering is significantly different to that of CePdAl where Ce(2) is fully Kondo screened, ending up with a single antiferromagnetic phase ($T_N = 2.7$ K) involving Ce(1) and Ce(3) [11]. The antiferromagnetic propagation vector of PrPdAl is also incommensurate with $\mathbf{k} = [1/2, 0, \tau]$ [16], resembling that of CePdAl regardless of their different

*pjsun@iphy.ac.cn

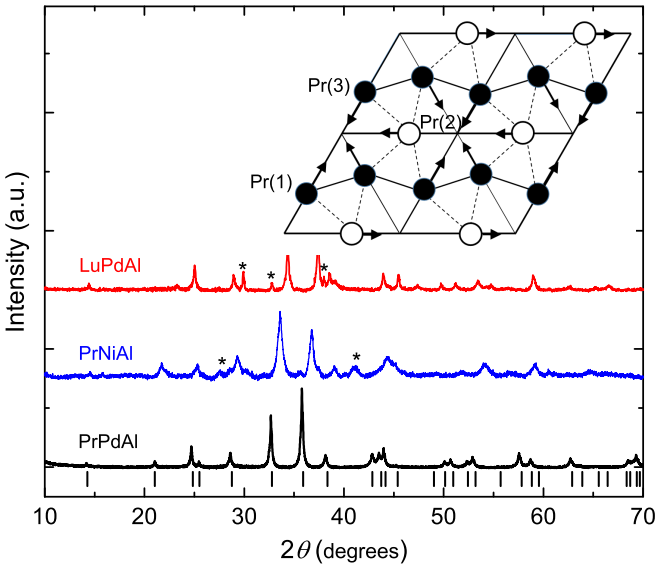

FIG. 1. X-ray powder diffraction patterns of the singlecrystalline PrPdAl, and the polycrystalline PrNiAl and LuPdAl. Vertical lines mark the calculated Bragg positions for PrPdAl and asterisks the unknown peaks for the later two compounds. Inset illustrates the kagome-like lattice of the Pr ions, where the in-plane spin structure of PrPdAl as obtained by neutron diffraction experiments is also shown [16,17]. Of the three Pr ions at $3f$ sites, Pr(1) and Pr(3) with larger moments are denoted by solid circle and Pr(2) with smaller moment by open circle.

spin characters, i.e., the XY-like and the Ising-like spins in PrPdAl and CePdAl, respectively. Interestingly, the magnetic Bragg peaks in PrPdAl are significantly split [17], showing three slightly different incommensurate propagation vector components of τ (i.e., 0.377, 0.401, and 0.418). Compared with Ce-based Kondo lattices with magnetic Kramers ions, Pr^{3+} ions with $4f^2$ configuration usually have non-Kramers doublet or singlet ground states. In the case of the non-Kramers doublet ground states, the two-channel Kondo effect may occur and the corresponding hybridization will lead to an excited $4f^1$ Kramers doublet. As a result, the Fermi-liquid ground state will not simply form without a phase transition [18]. Comprehensive investigations with these similarities and differences between the two compounds in mind will certainly shed light on the generic effects of spin frustrations in Kondo lattices, helping to elucidate the nature of emergent quantum stats therein.

In this work, we prepared a single crystal of PrPdAl for the first time and investigated its magnetic, transport, and thermodynamic properties down to very low temperatures. Long-range antiferromagnetic ordering with two successive phase transitions was confirmed, revealing an unusual magnetic anisotropy: The magnetically easy direction is not within the basal plane where the ordered magnetic moments reside in, but points along the c axis of the hexagonal lattice. Heavy-fermion-like behavior with an enhanced electronic specific-heat coefficient $\gamma \approx 940\,\mathrm{mJ/mol\ K^2}$ is observed with the corresponding Kadowaki-Woods (KW) ratio being, however, a factor-of-25 smaller compared with the common heavy-fermion compounds containing Ce ions. The Grüneisen ratio estimated from the low-temperature data of thermal expansion and specific heat shows enhanced values around T_{N2}, indicating its instability with respect to pressure. Along this line, in this work we also compared PrPdAl to PrNiAl, which is supposed to be a chemically pressurized analog of the former. Interestingly, PrNiAl shows only one antiferromagnetic transition at a considerably higher temperature $T_N = 6.9\,\mathrm{K}$, hinting at a partially lifted magnetic frustration relative to PrPdAl.

II. EXPERIMENTAL DETAILS

A single crystal of PrPdAl was grown by the Czochralski pulling method in an induction heating furnace. Because LaPdAl, which is supposed to be an appropriate nonmagnetic reference compound of PrPdAl with similar average atomic weight, forms in the orthorhombic LaNiAl-type structure, we instead prepared polycrystalline LuPdAl for this purpose by arc melting and a subsequent annealing at 800° C for one week. Moreover, to shed light on the magnetic instability of PrPdAl against pressure, polycrystalline PrNiAl was also prepared by arc melting. The proper ZrNiAl-type structure of the above three samples was confirmed by means of x-ray powder diffraction at room temperature. Specific heat was measured by the thermal relaxation method from room temperature down to 2 K in a commercial physical property measurement system (PPMS, Quantum Design) and further down to 0.3 K in a ^{3}He refrigerator by using a homemade thermal relaxation calorimeter. Resistivity was measured by using the standard four-probe method down to 2 K and 0.05 K in the PPMS and a ^{3}He - ^{4}He dilution refrigerator, respectively. Magnetic measurements were performed by using a vibrating sample magnetometer (VSM, Quantum Design) in the temperature range of 2 to 300 K, up to 7 T magnetic field. The same system was also employed in combination with a ^{3}He insert (iHelium3) to extend the magnetic measurements down to 0.5 K. Thermal expansion was measured using a miniaturized capacitance dilatometer down to 0.3 K in a ^{3}He refrigerator [19] by employing an Andeen-Hagerling 2500A capacitance bridge.

III. RESULTS

Figure 1 displays the x-ray powder diffraction patterns obtained at room temperature for PrPrAl, PrNiAl, and LuPdAl, which confirmed the identical crystal structure (ZrNiAl type) of these compounds, albeit with a few unknown peaks in the latter two. From these results, the unit cell parameters $a(c) = 7.204\ (4.221)$ Å for PrPdAl, $a(c) = 7.031\ (4.086)$ Å for PrNiAl, and $a(c) = 7.156\ (3.850)$ Å for LuPdAl were determined. The kagome-like lattice of Pr ions in the basal plane and the experimentally determined in-plane magnetic structure [16,17] of PrPdAl are also shown (Fig. 1, inset). All the magnetic moments are constrained in the basal plane, among which two-thirds at Pr(1) and Pr(3) sites form canted ferromagnetic chains, respectively, and couple antiferromagnetically between chains. Note that below T_{N2}, the reduced moments at Pr(2) take part in the magnetic ordering as well by forming ferromagnetic chains that couple to each other antiferromagnetically.

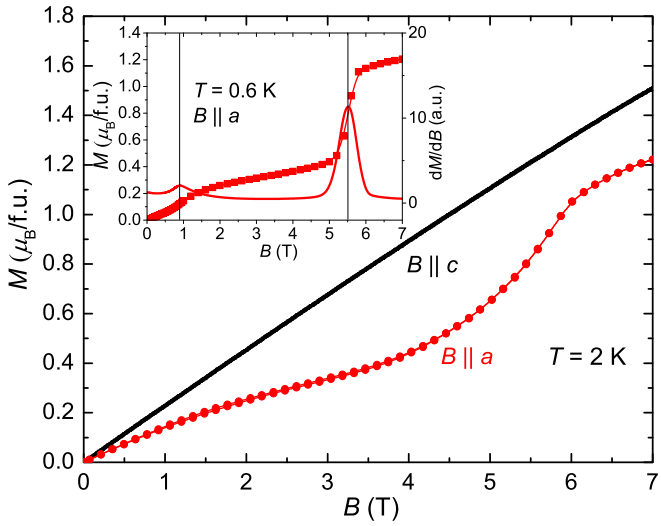

FIG. 2. Magnetization isotherms $M(B)$ measured at $T = 2$ K for PrPdAl with magnetic field applied along a and c axes. For $B \| a$, an S-shaped behavior indicative of a metamagnetic transition is observed, corroborating that the magnetic moments are constrained in the basal planes in the ordered phase, see the magnetic structure shown in Fig. 1, inset. Inset shows the $M(B)$ curve measured at $T = 0.6$ K for $B \| a$ in a ^{3}He insert and its field derivative.

Figure 2 shows the isothermal magnetization $M(B)$ of PrPdAl measured at $T = 2$ K with $B \parallel a$ and $B \parallel c$. For the in-plane magnetization measured along a, an S-shaped behavior is observed, indicative of a metamagnetic transition. By contrast, applying the transverse field along c causes the magnetization to increase smoothly without any significant feature, but larger $M(B)$ values. Extending the $M(B)$ measurements to below 2 K by using a ^{3}He insert confirmed the aforementioned in-plane metamagnetic transition: Except for a clear metamagnetic transition at 5.5 T, a weak anomaly at 0.9 T is also observed, see Fig. 2, inset for the $M(B)$ curve measured at $T = 0.6$ K and its field derivative. These distinct magnetization behaviors offer a further fingerprint of the in-plane arrangement of the Pr magnetic moments, as observed by neutron diffraction [16,17,20]. No indication of magnetization saturation is observed up to 7 T for both field orientations. For comparison, we note that in CePdAl the magnetic moments have Ising characters along c and consequently a couple of metamagnetic transitions appear in out-of-plane magnetization [21], whereas the in-plane $M(B)$ is one order-of-magnitude smaller [22]. The values of $M(B)$ attained at 7 T, 1.22 μ_B ($B \parallel a$) and 1.51 μ_B ($B \parallel c$), are less than half of the full moment of free Pr^{3+} ion, $gJ = 3.2$ μ_B, evidencing the important role of the crystal electric field (CEF) on the ground-state multiplet of Pr^{3+}.

The magnetic susceptibility $\chi = M/B$ is measured in an external field of 0.1 T applied along the a and c axes and shown in Fig. 3(a). No apparent difference can be found between zero-field-cooling and field-cooling measurements (not shown). Consistent with the results of $M(B)$ isotherms shown in Fig. 2, the values of the c-axis $\chi_c(T)$ are larger than those of $\chi_a(T)$ in the entire temperature range investigated (2–300 K). Such kinds of magnetic anisotropy with the ordered moments

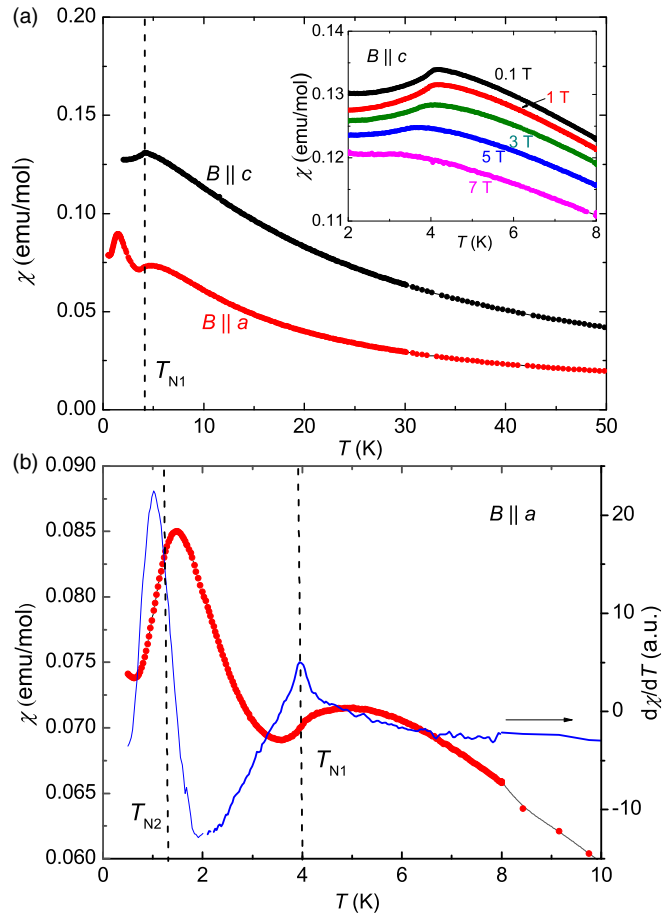

FIG. 3. (a) Magnetic susceptibility $\chi(T)$ measured in an external field of $B = 0.1$ T for PrPdAl. Note the larger values of c-axis $\chi(T)$ compared with those of a axis and the different signatures of antiferromagnetic ordering in them that point to enhanced spin frustrations in the basal plane, see text. Inset: The results of c-axis $\chi(T)$ measured in higher external fields reveal a decreasing T_{N1} with increasing field. (b) Low-temperature closeup of a-axis $\chi(T)$ and its temperature derivative (right axis). The derivative displays a sharp peak at T_{N1} that matches well to the corresponding anomaly observed in specific heat (to be discussed below). Here, $T_{N2} \approx 1.3$ K is marked according to the anomaly shown in the thermal expansion coefficient (see below), whereas the corresponding signature in specific heat appears to be rather broad.

residing in the basal plane and the magnetically easy axis pointing along c is uncommon and may hint at enhanced spin fluctuations in this compound. Indeed, similar behaviors were previously observed for a variety of ferromagnetic Kondo lattices with strong spin fluctuations [23]. In line with the potentially enhanced spin fluctuations in PrPdAl, the magnetic susceptibility within the basal plane, $\chi_a(T)$, shows a broad maximum at $T > T_{N1}$ and an abrupt drop at T_{N1} follows upon further cooling, as is evidenced by a sharp peak of $d\chi/dT$, see Fig. 3(b). This is different to $\chi_c(T)$ which displays a well-defined kink at $T_{N1} = 4.0$ K typical for the antiferromagnetic phase transition. These intriguing features observed in $\chi_a(T)$ are not uncommon for frustrated magnets. For instance, in $\chi(T)$ measured along the magnetically easy c axis of CePdAl, a broad maximum shows up at 4 K due to short-range spin

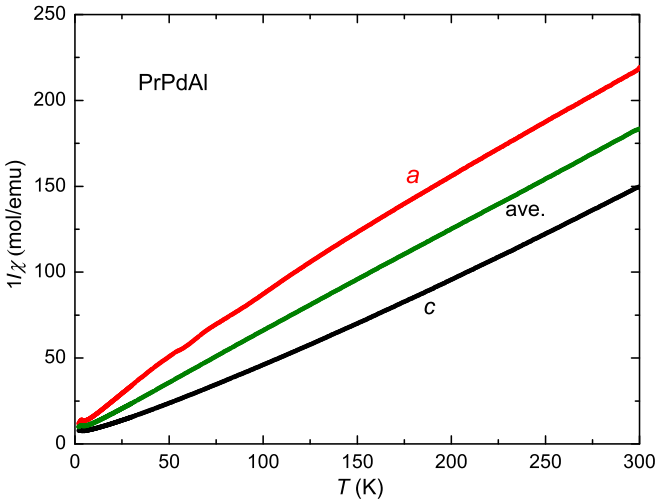

FIG. 4. The inverse magnetic susceptibility $\chi_a^{-1}(T)$ and $\chi_c^{-1}(T)$, as well as the calculated polycrystalline average $\chi_{\rm ave}^{-1}(T)$ of PrPdAl.

interactions, whereas the long-range antiferromagnetic phase transition takes place at 2.7 K, where $\chi(T)$ drops abruptly [24,25]. Furthermore, as seen from the inset of Fig. 3(a), the kink corresponding to $T_{\rm N1}$ decreases slightly with increasing external field, indicating the antiferromagnetic nature of the magnetic order. By extending the $\chi(T)$ measurements for $B \parallel a$ down to 0.5 K in a ^{3}He insert, one can clearly identify an anomaly due to the lower-temperature phase transition. Interestingly, it is even stronger than that at $T_{\rm N1}$, and its position ($T_{\rm N2} \approx 1.3$ K) is marked according to the anomaly shown in the thermal expansion coefficient (see below), rather than the peak positions of $d\chi(T)/dT$ (∼1 K) and $\chi(T)$ (∼1.5 K).

The inverse magnetic susceptibilities $\chi_a^{-1}(T)$, $\chi_c^{-1}(T)$, and the calculated polycrystalline average $\chi_{\rm ave}^{-1}(T)$, where $\chi_{\rm ave} = (2\chi_a + \chi_c)/3$, are displayed in Fig. 4. These data follow the modified Curie-Weiss function $\chi(T) - \chi_0 = C_0/(T - \theta_p)$ in the temperature window 200–300 K, yielding two considerably different paramagnetic Curie temperatures $\theta_p = -50$ K and 32.3 K for the a and c axes, respectively. The consequently obtained effective magnetic moments $\mu_{\rm eff} = 3.58\ \mu_B$ (a axis) and 3.60 μ_B (c axis) agree well with $\mu_{\rm eff} = g_J[J(J+1)]$ of the free Pr^{3+} ion, where the Landé factor $g_J = 0.8$ and $J = 4$. Here, χ_0 accounts for the Pauli paramagnetism of conduction electrons. The paramagnetic Curie temperature for $\chi_{\rm ave}(T)$ is $\theta_{\rm ave} = -13.7$ K, giving rise to a frustration parameter $|f| = |\theta_{\rm ave}|/T_{\rm N1} = 3.4$ that is moderately enhanced in response to the in-plane magnetic frustration.

The temperature-dependent specific heat $C(T)$ of PrPdAl and its nonmagnetic homolog LuPdAl is shown in Fig. 5(a), where $C(T)$ of PrNiAl is also shown for comparison. The magnetic contribution to PrPdAl, $C_m(T)$, estimated as the specific heat difference to LuPdAl, is shown on the right axis (solid circles). Several distinct features of $C_m(T)$ are readily observed: A sharp peak appears at 4 K due to onset of the antiferromagnetic phase at $T_{\rm N1}$, followed by a considerably extended high-temperature tail, which overlaps with a broad and shallow maximum originating from the CEF effect. Moreover, a small hump located between 1 and 2 K is also visible, which was already ascribed to the onset of

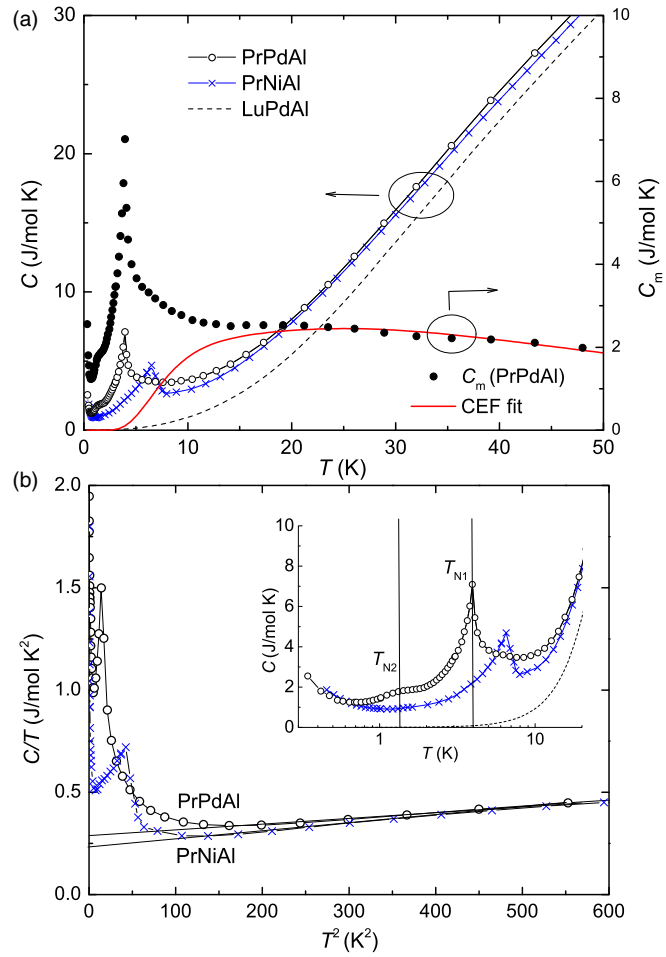

FIG. 5. (a) Temperature-dependent specific heat of PrPdAl and its nonmagnetic reference LuPdAl, as well as PrNiAl which is a chemically pressurized analog of PrPdAl. The magnetic contribution C_m to PrPdAl is approximated by its $C(T)$ difference to LuPdAl and shown on the right axis. The consequently obtained $C_m(T)$ is fitted by the Schottky contribution of a CEF-split Hund's rule multiplet of Pr^{3+} with a quasidoublet ground state and two excited singlets at $\Delta_1 = 30.8$ K and $\Delta_2 = 94.7$ K, respectively, see text. (b) C/T versus T^2 curves of PrPdAl and PrNiAl display a linear function between 15–30 K, yielding large γ values for both compounds. Inset shows the low-temperature closeup of $C(T)$ for the three relevant compounds in a semi-log representation.

a second antiferromagnetic phase at $T_{\rm N2}$ [16], see the low-temperature closeup shown as the semi-log representation in Fig. 5(b) inset. In the main panel of Fig. 5(b) we show the C/T versus T^2 for PrPdAl and its chemically pressurized analog PrNiAl. The linear variation of $C/T(T^2)$ can be observed between 15 and 30 K and extrapolates to large C/T values at zero temperature, i.e., 291 and 235 mJ/mol K^2 for PrPdAl and PrNiAl, respectively. Given the absence of apparent Kondo behaviors in the temperature-dependent resistivity (see below), such heavy-fermion-like behaviors offer clear evidence of strong spin fluctuations that are developed in the paramagnetic regime from geometrical frustrations in these compounds. Similar behaviors were observed in, for example, antiferromagnetic $GdInCu_4$ that has a frustrated face-centred cubic structure of local magnetic moments of Gd^{3+} ions [26].

However, we stress that the extended $C_m(T)$ tail at $T > T_{N1}$ and the CEF contribution nearby hinder a reliable application of the Debye's T-cube law. Below we would rather estimate the γ values from lower-temperature range to further take the strongly enhanced spin fluctuations deep in the ordered state into account.

The point symmetry of the Pr^{3+} ion at the $3f$ Wyckoff site is $m2m$, belonging to the point group C_{2v}. The corresponding CEF will split the Hund's rule multiplet ($J = 4$) into nine singlets [27,28]. The occurrence of magnetic ordering at low temperatures in both PrPdAl and PrNiAl indicates the CEF ground to be a magnetic quasidoublet with two nearly degenerate singlets. The broad maximum in $C_m(T)$ above 20 K for PrPdAl [Fig. 5(a)] can be well fitted by considering a CEF scheme with the quasi-doublet ground state, a first excited single at $\Delta_1 = 30.8$ K, and a second excited singlet at $\Delta_2 = 94.7$ K, see the red line. Here, the value of Δ_1 is smaller but comparable to that in PrNiAl, where $\Delta_1 = 50$ K has already been reported [27].

Figure 6(a) shows the data of C_m/T as a function of temperature for PrPdAl and PrNiAl. Except for the anomalies at T_{N1} and T_{N2}, the high-temperature tail at $T > T_{N1}$ in PrPdAl can be better observed to extend up to at least 20 K due to the enhanced spin fluctuations. The drastic increase of C_m/T values below 1 K is due to a Schottky-like contribution of Pr nuclear magnetic moments located in the internal field of local $4f$ electrons [29]. Combining a significant electronic term γT with a nuclear contribution $C_N T^{-2}$ to specific heat, one can reproduce this drastic upturn reasonably well, see the red line in Fig. 6(a) obtained for PrPdAl. From the fitting, one obtains $C_N = 259.1$ mJ K/mol and $\gamma \approx 940$ mJ/mol K^2, the second value is three times larger than that obtained from extrapolating C/T versus T^2 curve to zero temperature [Fig. 5(b)]. In Fig. 6(a), the C_m/T curve of PrPdAl with the nuclear part subtracted is also shown (solid circles), which does tend to saturate to the large γ value at zero temperature. Alternatively, one can also focus on the low-temperature tail of the C_m/T peak from below T_{N1} down to slightly above T_{N2}. By fitting this part to the following description, $C_m(T) = \gamma T + C_{sw} \cdot T^2 \exp(\frac{-\Delta_m}{k_B T})$, where the second term is due to the gapped spin waves, one obtains $\gamma \approx 960$ mJ/mol K^2, close to the aforementioned γ value, and $\Delta_m \approx 12.2$ K. The fitting result is shown as dotted line in Fig. 6(a).

To further characterize the low-temperature upturn in specific heat, in Fig. 6(b) we show the curves of C_m/T versus T measured in selected magnetic fields ($B \parallel a$) for PrPdAl. It can be seen that a small field of 1 T can smear out the broad anomaly at T_{N2}, while T_{N1} is rather robust and only drops to 3.5 K in $B = 5$ T. The specific heat upturn at $T < 1$ K is weakly enhanced in fields due to, at least partly, the enhanced nuclear contribution [29]. The values of C_N and γ obtained from the fitting [see solid lines in Fig. 6(b)] are shown in the inset of Fig. 6(b), where C_N increases smoothly with field and γ shows a nonmonotonic change within a window of enhanced values, i.e., 0.8–1.2 J/mol K^2. Here we note that, while we can safely conclude that the low-temperature γ values are significantly enhanced compared with that (291 mJ/mol K^2) obtained by extrapolating the C/T versus T^2 curve, there apparently exist inevitable uncertainties in these estimations due to the large nuclear contribution to specific heat.

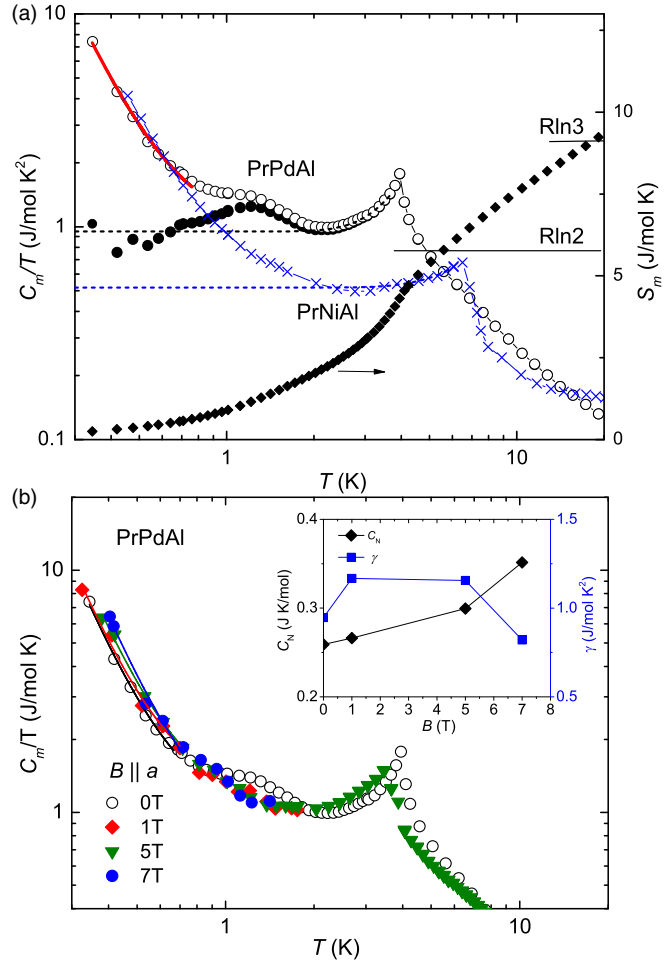

FIG. 6. (a) The magnetic specific heat shown as C_m/T versus T and the corresponding magnetic entropy $S_m(T)$ for PrPdAl. The red solid line at $T < 1$ K is a theoretical fit to C_m/T of PrPdAl by considering a linear-in-T (γT) and a nuclear $C_N T^{-2}$ contribution to the specific heat, see text. The solid circles are the values of C_m/T with the nuclear contribution subtracted, which tend to flatten out at the value of γ at zero temperature. C_m/T for PrNiAl (crosses) is also shown for comparison. The two dashed lines shown for PrPdAl and PrNiAl are calculations based on gapped spin waves, see text. (b) Low-temperature curves of C_m/T versus T measured in various magnetic fields ($B \parallel c$) in order for a better characterization of the nuclear and electronic contributions to PrPdAl. Inset shows the values of C_N and γ as a function of field that are obtained in fitting the low-temperature upturns.

The C_m/T versus T curve for PrNiAl, which is also shown in Fig. 6(a), reveals a broadened peak at $T_N = 6.9$ K due to the onset of its antiferromagnetic order, in agreement with the reported data [27]. Here $C(T)$ of LuNiAl as reported in Ref. [27] is used as a nonmagnetic reference to account for the phonon contribution. At $T < T_N$ and upon cooling, C_m/T displays a slow decrease down to about 3 K, below which the nuclear specific heat dominates. Similar to the analysis performed for PrPdAl, C_m/T from below T_N down to 3 K is fitted by taking into account an electronic and a gapped spin-wave term, see

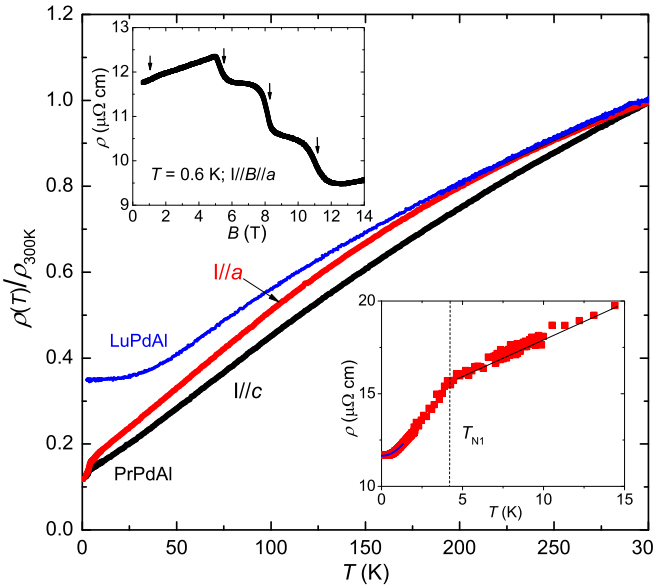

FIG. 7. Temperature dependence of the normalized electrical resistivity $\rho(T)/\rho_{300K}$ of PrPdAl measured with current flowing along a and c axes and that of polycrystalline LuPdAl for comparison. Upper inset shows the isothermal magnetoresistance measured at 0.6 K up to 14 T with both current and field applied along the a axis. Lower inset shows the a-axis $\rho(T)$ for $T < 15$ K, where the Fermi liquid description, $\rho = \rho_0 + AT^2$, is applied to the low-temperature part at $T < 1.2$ K. The solid line illustrates the T-linear resistivity variation that can extend all the way up to 100 K.

the dashed line in Fig. 6(a). The therefore obtained electronic specific heat coefficient $\gamma \approx 528$ mJ/mol K^2 is much larger than that obtained by extrapolating $C/T(T^2)$ linearly down to zero temperature [Fig. 5(b)].

The magnetic entropy $S_m(T)$ of PrPdAl is calculated by integrating C_m/T with respect to T with the nuclear contribution subtracted and shown in Fig. 6(a) also. At $T = T_{N1}$, $S_m(T)$ reaches 4.25 J/mol K, i.e., 73.7% of Rln2, evidencing again a quasidoublet CEF ground state. The considerably reduced entropy relative to Rln2 is consistent with the fact that strong spin fluctuations are already present at temperatures much higher than T_{N1}, as is reflected by the large γ value estimated from paramagnetic regime [Fig. 5(b)]. The value of $S_m(T)$ does not level off to Rln2 at $T > T_{N1}$; it instead increases continuously with warming and attains $Rln3$ already around 20 K due to the low energy of the first excited CEF level, i.e., $\Delta_1 = 30.8$ K.

The electrical resistivity $\rho(T)$, after being normalized to its room temperature value, is shown in Fig. 7 for PrPdAl and LuPdAl. The residual resistivity ratio (ρ_{300K}/ρ_{2K}) is about 8 for both a and c axes of the first, moderately larger than that of the second, which is about 2.8, implying a better quality of the single crystal samples. The resistivity anisotropy of PrPdAl is not strong but clearly detectable, with larger magnetic contribution for the a axis that is presumably related to the frustrated moments within the basal plane. Likewise, a sublinear $\rho(T)$ behavior over a wide temperature range from about 100 K down to T_{N1} is better observed along a rather than along c axis, below which an abrupt drop occurs due to the onset of the ordered state, see the lower inset. By contrast, $\rho(T)$ of LuPdAl exhibits a typical metallic behavior with negative curvature over a wide temperature range that originates from strong s-d interband scattering. No apparent behaviors of Kondo effect characterised by $-\ln T$ dependence can be observed for PrPdAl, indicating a weaker energy scale of the Kondo effect relative to that of the spin fluctuations induced by frustration. The Fermi-liquid behavior characterized by T-square dependence can be observed below 1.2 K (see lower inset), with the prefactor $A = 0.38(\pm 0.05)$ $\mu\Omega$cm/K^2. In the upper inset of Fig. 7, we show the magnetoresistance isotherm measured at 0.6 K with both the current and field applied along the a axis to confirm the metamagnetic behaviors observed in low-temperature isothermal magnetization (Fig. 2, inset). One can identify three metamagnetic transitions by abrupt drops at $B \approx 5.5$, 8.3, and 11.0 T, as well as a small hump at $\approx$1 T. The appearance of multiple field-induced phase transitions indicates a competition between the Zeeman energy and the exchange interaction beyond the nn Pr moments. Given the in-plane ordered moments and the partial ordering of PrPdAl that are similar to those of HoAgGe [10], this compound deserves further investigation to elucidate whether it may exhibit kagome spin ice behaviors as observed in HoAgGe.

The thermal expansion of PrPdAl was measured along both the a and c axes by using a sample with dimension of $0.8 \times 1.2 \times 1.3$ mm^3. The relative length changes $(\Delta l/l)_a$ and $(\Delta l/l)_c$, as well as the estimated relative volume change $\Delta V/V = 2(\Delta l/l)_a + (\Delta l/l)_c$ are shown in Fig. 8(a) for $T < 8$ K. This is the temperature window where the thermal expansions of PrPdAl are expected to be dominated by thermodynamics of the Pr $4f$ electrons, as referred to the experimental results of the low-temperature specific heat [Fig. 5(a)]. The coefficients of linear and volume thermal expansions, $\alpha = (1/l)dl/dT$ and $\beta = 2\alpha_a + \alpha_c$, after being divided by T, are shown in Fig. 8(b). Reflecting the magnetocrystalline anisotropy as observed in magnetic properties [Figs. 2 and 3(a)], the thermal expansion is also anisotropic with α_a and α_c being positive and negative, respectively. At $T_{N1} = 4$ K, α_a (α_c) reveals a sharp positive (negative) peak, manifesting the onset of the antiferromagnetic phase. Here, the lattice volume reveals a significant contraction at T_{N1}, see Fig. 8(a). This behavior is known as the exchange striction [30] that occurs commonly along with an antiferromagnetic ordering. Observation of a significant exchange striction along a, rather c, is in line with the fact that the $4f$ magnetic moments reside in the hexagonal basal planes. Markedly, a positive and a negative peak can also be observed at $T \approx 1.3$ K in $\alpha_a(T)/T$ and $\alpha_c(T)/T$, respectively, which are taken as clear signatures of magnetic ordering at T_{N2}. The dilatometric characteristics of the phase transitions at T_{N1} and T_{N2} are similar, albeit those for T_{N2} being broadened, offering an additional evidence that the phase transition at T_{N2} is of antiferromagnetic nature like that at T_{N1}.

The thermal expansion coefficient can be related to the specific heat thermodynamically via the Grüneisen parameter, $\Gamma = B_T V_m \beta/C$, where B_T is the isothermal bulk modulus and V_m the molar volume. Here we approximate B_T from the density d and the mean phonon velocity v, $B_T = dv^2$. The mean phonon velocity is estimated from the Debye temperature θ_D, namely $v = (k_B\theta_D/\hbar)(V_{atom}/6\pi^2)^{1/3}$, where k_B is the Boltzmann constant and V_{atom} the average volume per atom. Using

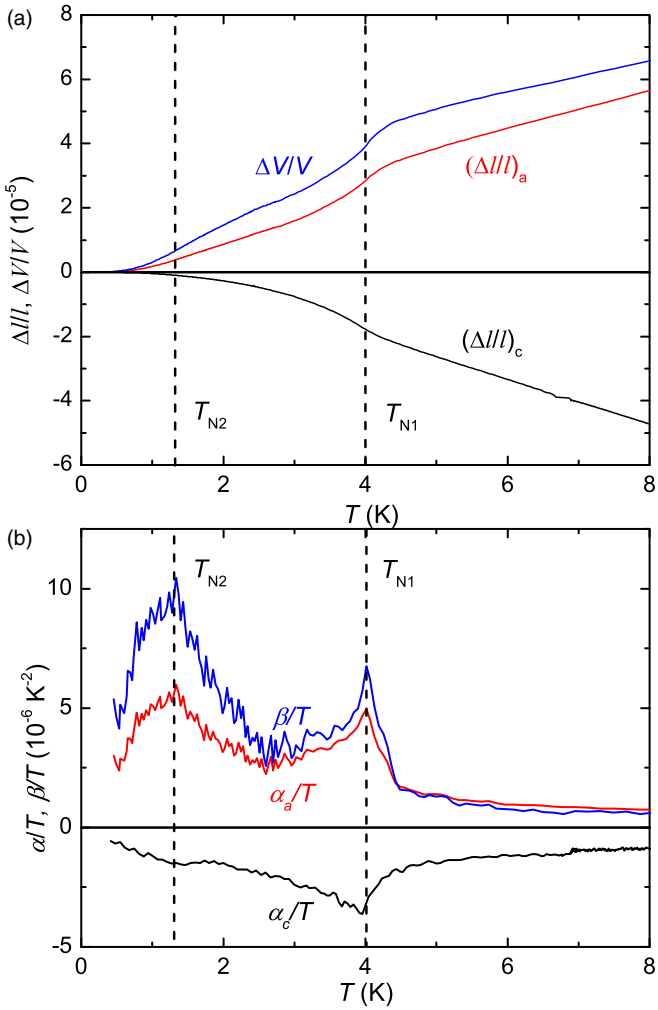

FIG. 8. (a) Temperature dependencies of the relative length changes $(\Delta l/l)_a$ and $(\Delta l/l)_c$, and the estimated relative volume change $\Delta V/V$ of the singlecrystalline PrPdAl. (b) The corresponding coefficients of linear and volume thermal expansions divided by temperature. The α/T profiles at T_{N1} and T_{N2} are similar, albeit the much broadened feature at the second of these. This serves as one piece of evidence that the weak ordering at T_{N2} is also antiferromagnetic.

the Debye temperature of $\theta_D = 276$ K that is evaluated from the specific heat data, we can get $B_T = 47.6$ GPa for PrPdAl. As shown in Fig. 9, while the calculated $\Gamma(T)$ has a weak anomaly at T_{N1}, a broad and enhanced maximum at around T_{N2} is observed, with the Γ values being as large as those of typical heavy fermion compounds such as $CeCu_6$ [31]. Such behaviors are simply caused by the much enhanced anomaly of the volume thermal expansion coefficient at T_{N2} relative to that of specific heat. Because the Grüneisen parameter measures pressure dependence of the characteristic energy scale of a certain thermodynamic system, the enhanced values of Γ around T_{N2} indicate an enhanced instability of this ordering with respect to pressure. Indeed, PrNiAl, which is a chemically pressurized analog of PrPdAl, has only one magnetic order at a considerably higher temperature $T_N = 6.9$ K and no subsequent order is observed. How the two antiferromagnetic transitions in PrPdAl evolve into one with pressure appears to be a very interesting project for future study.

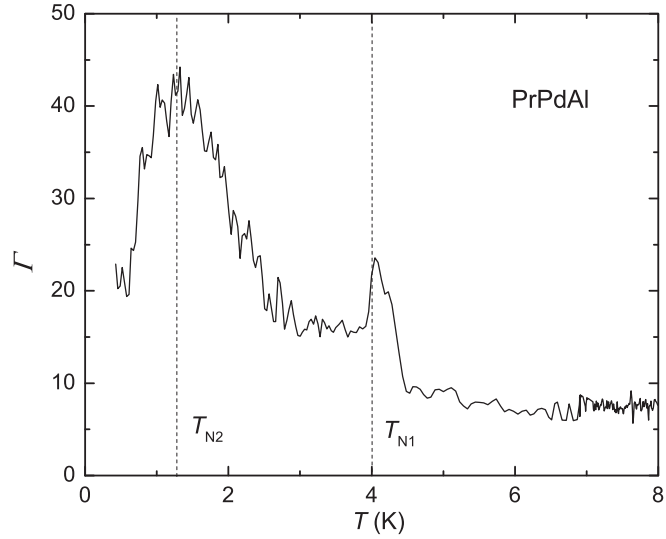

FIG. 9. Grüneisen parameter as a function of temperature for PrPdAl. A broad maximum is observed around T_{N2}, indicating an enhanced instability of the lower-temperature antiferromagnetic phase against pressure, whereas only a much weaker anomaly is observed at T_{N1}.

IV. DISCUSSION

Based on the electronic specific-heat coefficient $\gamma = 940$ mJ/mol K^2 and the resistivity coefficient A of the quadratic-in-temperature term, one can readily estimate the Kadowaki-Woods (KW) ratio $A/\gamma^2 = 0.4\ \mu\Omega \cdot \text{cm}(\text{K} \cdot \text{mol/J})^2$ for PrPdAl. This ratio is a factor-of-25 smaller than that of common heavy-fermion compounds with doublet or quasidoublet magnetic ground states [32]. We attribute the strongly reduced KW ratio to the unusually enhanced value of γ arising from the strong quantum fluctuations of Pr moments underpinned by geometrical frustration, in addition to the weak Kondo effect acting on the Pr^{3+} ions. By contrast, the Ce-based analog CePdAl with $\gamma = 270$ mJ/mol K^2 and $A = 2.3\ \mu\Omega$ cm/T^2 [25] has a normal KW ratio that falls well into the expectation for typical heavy-fermion compounds. As distinct features distinguishing the two systems, Ce^{3+} is a Kramers ion and the frustrated Ce(2) has been fully Kondo screened in CePdAl, whereas Pr^{3+} in PrPdAl is a magnetic non-Kramers ion and the frustrated Pr(2) remains partially screened and orders below T_{N2}. In fact, theoretically, in Pr-based magnetic compounds with $4f$-conduction band hybridization, the two-channel Kondo effect is expected to cause a quantum critical ground state [18] that is different to the Fermi liquid expected in Ce-based compounds in case no magnetic order is present. Whether the difference in ground-state behaviors between CePdAl and PrPdAl is partially due to the weak two-channel Kondo effect acting on PrPdAl remains an interesting question.

Resembling PrPdAl, the $4f$ moments of PrNiAl reside in the basal plane as well, and the antiferromagnetic propagation vector is alike, being $\mathbf{k} = (1/2, 0, \tau)$ with $\tau = 0.41$ [20,33]. However, as already mentioned, PrNiAl shows only one antiferromagnetic transition at a considerably higher temperature $T_N = 6.9$ K [5,27], in spite of the chemical pressure effect realized by the Ni replacement of Pd. The different mag-

netic properties of the two highly related Pr-based compounds point to a partially released spin frustration in PrNiAl, which we propose can be qualitatively traced by the slightly different lattice parameters of the two compounds. While both PrPdAl and PrNiAl crystalize in the hexagonal ZrNiAl-type structure, the low-temperature lattice parameters are $a(c) = 7.1631(4.2182)$ Å (obtained at $T = 8$ K, cf. Ref. [17]) for PrPdAl and $a(c) = 7.003(4.085)$ Å ($T = 13$ K, cf. Ref. [5]) for PrNiAl. The consequently obtained low-temperature c/a ratios are 0.589 and 0.583 for PrPdAl and PrNiAl, respectively. In addition, the room-temperature c/a ratios as obtained from the analysis of our x-ray diffraction patterns are 0.586 and 0.581 for the two compounds. The slightly larger c/a ratio of PrPdAl indicates an enhanced interlayer distance, adding more importance to the kagome-like frustration within the basal plane. Inversely, a reduced c/a ratio tends to ruin the in-plane frustration by enhancing interlayer interactions. To corroborate this argument, here we note another Pr-based homologue, PrCuAl [34]. In PrCuAl, the ratio $c/a = 0.575$ ($T = 12$ K) is even smaller, suggesting a further reduced spin frustration. Accordingly, PrCuAl orders not only at a higher temperature $T_N = 7.9$ K, but with all the Pr $4f$ moments involved in a commensurate vector $\mathbf{k} = (1/3, 1/3.1/3)$ [34]. Here, the three Pr ions on the $3f$ sites are magnetically equivalent, all with large magnetic moments of about 3.0 μ_B.

As to the large C/T values associated with enhanced quantum fluctuations of frustrated spins, recently we observed similar behaviors in a quasi-one-dimensional Kondo lattice $CeAu_2In_4$ [35]. Likewise, a largely reduced KW ratio is observed in $CeAu_2In_4$, pointing to the enhancement of C/T due to spin fluctuations arising from low dimensionality. In addition, as long as the Pr-based frustrated Kondo lattice is concerned, pyrochlore iridate $Pr_2Ir_2O_7$ offers another good reference. In that case, long-rang magnetic order is not observed, and the partially Kondo-screened $4f$ moments are proposed to form a metallic spin liquid in the ground state [36].

V. SUMMARY

To summarize, we investigate the low-temperature magnetic, transport, and thermodynamic properties of single crystalline PrPdAl for the first time. These results reveal two successive antiferromagnetic phases below $T_{N1} = 4$ K and $T_{N2} \approx 1.3$ K with rather different thermodynamics, and heavy-fermion-like ground-state properties with enhanced γ values. Several prominent features emerge as a consequence of the competition involving multiple energy scales of the Kondo effect, RKKY interaction, and spin frustration. (1) The magnetically easy axis points along c, transverse to the hexagonal basal plane where the ordered $4f$ moments reside in. (2) The low-temperature values of C/T appear to be large due probably to the enhanced spin frustrations, with the Kadowaki-Woods ratio being much smaller compared to that of typical heavy fermion compounds. (3) Compared to CePdAl where the frustrated one-third moment Ce(2) is fully Kondo screened, PrPdAl displays a subsequent order from frustrated Pr(2), albeit the largely reduced moment. How the two-channel Kondo effect acting on Pr^{3+} ions, in comparison to the conventional magnetic Kondo effect on Ce^{3+}, is involved remains a challenging issue. (4) The Grüneisen ratio analysis based on thermal expansion and specific heat measurements reveals enhanced values around the lower-temperature ordering at T_{N2}, indicating its instability against pressure. Along this line, intriguingly, PrNiAl shows only one antiferromagnetic transition at $T_N = 6.9$ K, hinting at a partially released frustration. Given the great chemical tunability of the ZrNiAl-type compounds, how the two successive magnetic orderings and heavy-fermion-like behaviors react on chemical pressure realized by replacing Pd by Ni, or hydrostatic pressure applied on PrPdAl, promises a significant follow-up to clarify the interplay between spin frustration, RKKY interaction, and the Kondo effect of two-channel type.

ACKNOWLEDGMENTS

This work was supported by the National Natural Science Foundation of China (Grants No. 11774404, No. 52088101, and No. 12141002), the National Key R&D Program of China (Grant No. 2017YFA0303100), and the Chinese Academy of Sciences through the Scientific Instrument Developing Project (Grant No. ZDKYYQ20210003) and the Strategic Priority Research Program (Grant No. XDB33000000).

[1] P. Coleman and A. H. Nevidomskyy, J. Low Temp. Phys. **161**, 182 (2010).
[2] C. Lacroix, J. Phys. Soc. Jpn. **79**, 011008 (2010).
[3] S. Paschen and Q. Si, Nat. Rev. Phys. **3**, 9 (2021).
[4] R. Pöttgen and B. Chevalier, Z. Naturforsch. B **70**, 289 (2015).
[5] G. Ehlers and H. Maletta, Z. Phys. B **101**, 317 (1997).
[6] Q. Si, Phys. Status Solidi B **247**, 476 (2010).
[7] H. Zhao, J. Zhang, M. Lyu, S. Bachus, Y. Tokiwa, P. Gegenwart, S. Zhang, J. G. Cheng, Y-f. Yang, G. F. Chen, Y. Isikawa, Q. Si, F. Steglich, and P. Sun, Nat. Phys. **15**, 1261 (2019).
[8] Y. Tokiwa, Christian Stingl, M.-S. Kim, T. Takabatake, and P. Gegenwart, Sci. Adv. **1**, e1500001 (2015).
[9] Y. Tokiwa, M. Garst, P. Gegenwart, S. L. Bud'ko, and P. C. Canfield, Phys. Rev. Lett. **111**, 116401 (2013).
[10] K. Zhao, H. Deng, H. Chen, K. A. Ross, V. Petříček, G. Günther, M. Russina, V. Hutanu, and P. Gegenwart, Science **367**, 1218 (2020).
[11] A Dönni, G. Ehlers, H. Maletta, P. Fischer, H. Kitazawa, and M. Zolliker, J. Phys.: Condens. Matter **8**, 11213 (1996).
[12] C. Schank, F. Jährling, L. Luo, A. Grauel, C. Wassilew, R. Borth, G. Olesch, C. D. Brell, C. Geibel, and F. Steglich, J. Alloys Compd. **207-208**, 329 (1994).
[13] H. Kitazawa, A. Matsushita, T. Matsumoto, and T. Suzuki, Phys. B: Condens. Matter **199-200**, 28 (1994).
[14] V. Fritsch, N. Bagrets, G. Goll, W. Kittler, M. J. Wolf, K. Grube, C.-L. Huang, and H. V. Löhneysen, Phys. Rev. B **89**, 054416 (2014).
[15] M. Núñez-Regueiro, C. Lacroix, and B. Canals, Physica C **282-287**, 1885 (1997).

[16] L. Keller, A. Dönni, H. Kitazawa, J. Tang, F. Fauth, and M. Zolliker, Phys. B **241-243**, 660 (1997).
[17] L. Keller, A. Dönni, and H. Kitazawa, Phys. B: Condens. Matter **276-278**, 672 (2000).
[18] R. Flint and T. Senthil, Phys. Rev. B **87**, 125147 (2013).
[19] R. Küchler, T. Bauer, M. Brando, and F. Steglich, Rev. Sci. Instrum. **83**, 095102 (2012).
[20] P. Javorsky P. Burlet, V. Sechovský, R. R. Arons, E. Ressouche, and G. Lapertot, Phys. B: Condens. Matter **234-236**, 665 (1997).
[21] T. Goto, S. Hane, K. Umeo, T. Takabatake, and Y. Isikawa, J. Phys. Chem. Solids **63**, 1159 (2002).
[22] Y. Isikawa, T. Mizushima, N. Fukushima, T. Kuwai, J. Sakurai, and H. Kitazawa, J. Phys. Soc. Jpn. **65** (Suppl. B), 117 (1996).
[23] D. Hafner, B. K. Rai, J. Banda, K. Kliemt, C. Krellner, J. Sichelschmidt, E. Morosan, C. Geibel, and M. Brando, Phys. Rev. B **99**, 201109(R) (2019).
[24] V. Fritsch, S. Lucas, Z. Huesges, A. Sakai, W. Kittler, C. Taubenheim, S. Woitschach, B. Pedersen, K. Grube, B. Schmidt, P. Gegenwart, O. Stockert, and H. V. Löhneysen, J. Phys.: Conf. Ser. **807**, 032003 (2017).
[25] H. Zhao, J. Zhang, S. Hu, Y. Isikawa, J. Luo, F. Steglich, and P. Sun, Phys. Rev. B **94**, 235131 (2016).
[26] H. Nakamura, K. Ito, H. Wada, and M. Shiga, Phys. B: Condens. Matter **186-188**, 633 (1993).
[27] P. Javorský, H. Mutka, and H. Nakotte, Appl. Phys. A **74**, s658 (2002).
[28] N. C. Tuan, V. Sechovský, M. Diviš, P. Svoboda, H. Nakotte, F. R. de Boer, and N. H. Kim-Ngan, J. Appl. Phys. **73**, 5677 (1993).
[29] A. K. Pathak, D. Paudyal, Y. Mudryk, K. A. Gschneidner, Jr., and V. K. Pecharsky, Phys. Rev. Lett. **110**, 186405 (2013).
[30] M. Doerr, M. Rotter, and A. Lindbaum, Adv. Phys. **54**, 1 (2005).
[31] A. de Visser, A. Lacerda, P. Haen, J. Flouquet, F. E. Kayzel, and J. J. M. Franse, Phys. Rev. B **39**, 11301 (1989).
[32] K. Kadowaki and S. Woods, Solid State Commun. **58**, 507 (1986).
[33] G. Ehlers and H. Maletta, Phys. B: Condens. Matter **234-236**, 667 (1997).
[34] P. Javorský, J. Kaštil, and O. Isnard, J. Phys.: Conf. Ser. **200**, 032027 (2010).
[35] M. Lyu, H. Zhao, J. Zhang, Z. Wang, S. Zhang, and P. Sun, Chin. Phys. B **30**, 087101 (2021).
[36] S. Nakatsuji, Y. Machida, Y. Maeno, T. Tayama, T. Sakakibara, J. van Duijn, L. Balicas, J. N. Millican, R. T. Macaluso, and J. Y. Chan, Phys. Rev. Lett. **96**, 087204 (2006).